2010 International Conference on Biology, Environment and Chemistry
IPCBEE vol.1 (2011) © (2011) IACSIT Press, Singapore

Enhancement of heat Transfer by a Swirling Element of Radiant Tube in Cracking Furnace

Lijun Zhang, Yuanyi Yang
Department of chemical Engineering
Beijing University of Chemical Technology
Beijing, CHINA
Zhanglj.bjhy@sinopec.com

Guoqing Wang
Department of ethylene pyrolysis
Beijing Research Institute of Chemical Industry
Beijing, Chaoyang 100013, CHINA
Wanggq.bjhy@sinopec.com

Abstract – **The heat transfer of Swirling Element of Radiant Tube (SERT) has been compared to that of bare tubes in the laboratory experiments and industrial experiments, this comparison also has been performed using CFD simulation. Result shows the plug flow is switched to swirl flow by SERT but the swirl flow is decaying along the tube. It is confirmed that thermal efficiency for SERT is superior to bare tube due to the SERT has a significant effect on the inside heat transfer coefficient. The decrease of TMT in industrial experiments demonstrates that the SERT can intensify heat transfer and extend the run length of the furnace.**

***Index Terms – swirl flow, heat transfer, CFD simulation, cracking furnace*.**

I. INTRODUCTION

Ethylene production is a cornerstone of the chemical process industry. Thermal cracking is one of the most important processes in the petrochemical industry converting a hydrocarbon feedstock into more valuable products such as ethylene and propylene, and it is an endothermic process that takes place in the cracking furnaces. A cracking furnace typically consists of a long, relatively narrow furnace (radiant firebox) containing a large number of coils (process tubes) suspended in the firebox and a large number of gas burners. The purpose of the cracking furnace is to heat the process fluid (raw chemical feed stock) to a high cracking temperature to selectively produce olefins while minimizing coking rate[1,2].

In the furnace, the heat transfer to reactor tubes is mainly due to radiation from the furnace refractory walls with temperature up to 1500 K and to radiation from the flue gas with temperature up to 2100 K; the heat transfer to process fluid is mainly due to convection from the tube walls with temperature of around 1300K[3]. In the meantime, the thermal cracking reaction occurs in the process fluid and the target products such as ethylene and propylene are produced, however, the undesired products such as coke are also produced. The coke deposits of a few millimeters to centimeters in thickness lead to poor heat transfer. In order to retain the same process temperature and hence the same conversion, plant operators have to raise the temperature of metal tube (TMT) continuously, which often leads to more rapid coke formation and hot spots on the tube wall. The coke build-up also increases the pressure drop, which results in lower ethylene yield. With time, this accumulation of coke forces the operator to shut down the furnace either on TMT or on pressure drop [4-6]. Hot spots can damage the tube material and lead to local excessive coke formation, thus reducing the normal run length of the production cycle. Uniform tempera-tures are recommended, not only in the axial direction of the tubes, but also along the tube perimeter. On the one hand, since heat is mainly transmitted by radiation at the high temperatures required by the operation, special care has to be taken to maximize the incidence of direct radiation from the flames on the coils and to minimize the shadow effects; on the other hand, forced convection such as swirl flow by device installed in the tube in the process fluid can also improve the uniform temperature.

It is well known that swirl flow in tubes may be classified into two essential types [7]: continuous swirl flow and decay-ing swirl flow. In continuous swirl flow, the swirling motion persists over the whole length of the tube, but the pressure drop is high such as MERT[8], while in the decaying swirl flow, the swirl is generated at the several sections of the tube and decays along the flow path, the pressure drop is low. We design the device called Swirling Element of Radiant Tube (SERT), which is installed in the tube, to force the plug flow to decaying swirl flow and then raise the rate of heat transfer.

This study reports on a laboratory experiments to see whether or not heat transfer can be enhanced by SERT, and in this paper the CFD simulation of the tube with SERT and industrial application also has been done, we also inspect whether or not these results can coincide with the result of industrial experiments.

II. EXPERIMENTS AND CFD SIMULATION

A general arrangement of the experimental equipment used in this laboratory experiment is shown in Fig. 1. Initially air enters the flow stabilizer by a centrifugal blower. Prior to entry into the flow stabilizer, the flow rate of air is measured by an orifice meter. And then air flow enters the flow straighten section and test section in turn. The straighten section was used to obtain air flow which has as little disturbance as possible before enters the SERT. Figure 2 shows the form of the SERT, The twisted angle of the insert vane can vary between 100° and 360°. The thickness of the vane is approximately the same as the coil tube. Every

cross section of the insert is divided into two passages. The connection between the surface of the vane and the surface of the coil piece has the shape of a concave circular arc. This type of shape minimizes the eddy formation at any point in the passage, and reduces flow resistance and hence pressure drop.

At the upstream of the test tube, a piece of SERT which generates swirl flow is installed. The test tube was prepared from a commercial transparent plastic pipe of 62 mm inner diameter. The speed of air in the test pipe was inspected by the laser Doppler anemometry. The data from the laser Doppler anemometry was collected in the data collection and then was analyzed by the computer.

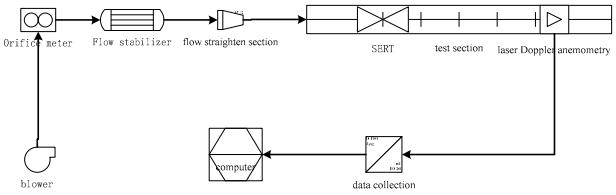

Figure 1. The flow chart of experimental equipment

Besides experimental study, the CFD simulation of swirl flow is also developed. The flow in the tube where the SERT was installed is simulated using commercial CFD codes FLUENT. The geometry of the tube is built and boundary condition in accordance with experimental data is given using GAMBIT. In this work a typical integration grid contains about 100000 volume cells depending on SERT and tube geometry.

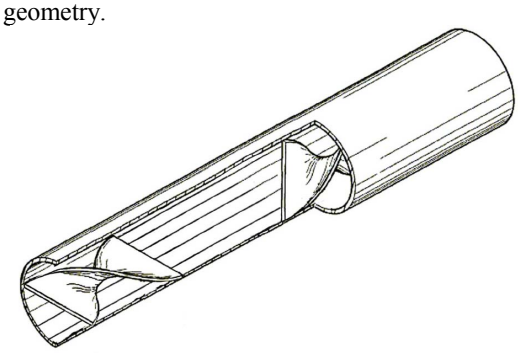

Figure 2. The sketch map of the SERT

The calculation of the steady-state flow field is based on the compressible Reynolds-averaged Navier-Stokes equations (RANS). Due to the time averaging of the equations, a closure model is required to account for turbulence, in addition to the total continuity, momentum and energy equations. In this work the standard k- ε turbulence model is applied. Omitting an explicit notation indicating that the variables are Reynolds-averaged, the resulting equations can be written as:

Continuity equation: $$\frac{\partial}{\partial x_i}\left(\rho u_i\right) = 0 \tag{1}$$

Momentum equation: $$\frac{\partial}{\partial x_j}\left(\rho u_i u_j\right) = \frac{\partial p_{eff}}{\partial x_i} + \frac{\partial}{\partial x_i}\left[\mu_{eff}\left(\frac{\partial u_i}{\partial x_j} + \frac{\partial u_j}{\partial x_i} - \frac{2}{3}\delta_{ij}\frac{\partial u_l}{\partial x_l}\right)\right] \tag{2}$$

k-equation: $$\frac{\partial}{\partial x_i}\left(\rho k u_i\right) = \frac{\partial}{\partial x_j}\left(\alpha_k \mu_{eff}\frac{\partial k}{\partial x_j}\right) + G_k + G_b - \rho\varepsilon \tag{3}$$

ε -equation: $$\frac{\partial}{\partial x_i}\left(\rho\varepsilon u_i\right) = \frac{\partial}{\partial x_j}\left(\alpha_\varepsilon \mu_{eff}\frac{\partial \varepsilon}{\partial x_j}\right) + C_{1\varepsilon}\frac{\varepsilon}{k}\left(G_k + C_{3\varepsilon}G_b\right) - C_{2\varepsilon}^{*}\rho\frac{\varepsilon^2}{k} \tag{4}$$

Energy equation: $$\frac{\partial}{\partial x_i}\left[u_i\left(\rho E + P\right)\right] = \frac{\partial}{\partial x_j}\left(\lambda_{eff}\frac{\partial T}{\partial x_j} + \sum_{i=1}^{N} h_i J_{i,j} + u_i \mu_{eff}\left[\left(\frac{\partial u_j}{\partial x_i} + \frac{\partial u_i}{\partial x_j}\right) - \frac{2}{3}\frac{\partial u_l}{\partial x_l}\delta_{i,j}\right]\right) + S_{chem} + S_{rad} \tag{5}$$

Where:

$$\mu_{eff} = \mu + \mu_t \tag{6}$$

$$p_{eff} = p + \frac{2}{3}\rho k \tag{7}$$

$$C_{1\varepsilon} = 1.42 - \frac{\eta\left(1-\eta/\eta_0\right)}{1+\beta\eta^3} \tag{8}$$

$$C_{2\varepsilon}^{*} = C_{2\varepsilon} + \frac{C_\eta \eta^3\left(1-\eta/\eta_0\right)}{1+\beta\eta^3} \tag{9}$$

$$C_{3\varepsilon} = \tanh\left|\frac{u_3}{\sqrt{u_1^2+u_2^2}}\right| \tag{10}$$

$$G_k = \mu_t\left[\left(\frac{\partial u_i}{\partial x_j} + \frac{\partial u_j}{\partial x_i}\right) - \frac{2}{3}\frac{\partial u_l}{\partial x_l}\delta_{ij}\right]\frac{\partial u_i}{\partial x_j} \tag{11}$$

$$G_b = -\beta g_i \frac{\mu_t}{\mathrm{Pr}_t}\frac{\partial T}{\partial x_i} \tag{12}$$

$$\lambda_{eff} = \alpha c_p \mu_{eff} \tag{13}$$

$$\eta = \frac{k}{\varepsilon}\sqrt{2S_{ij}S_{ij}} \tag{14}$$

$$S_{ij} = \frac{1}{2}\left(\frac{\partial u_i}{\partial x_j} + \frac{\partial u_j}{\partial x_i}\right) \tag{15}$$

$$E = h - \frac{p}{\rho} + \frac{u^2}{2} \tag{16}$$

$$h = \sum_{i=1}^{N} Y_i h_i \tag{17}$$

$$h_i = \int_{T_{ref}}^{T} c_{p,i} dT \tag{18}$$

The governing equations for the conservation of mass, momentum, energy, turbulence, are solved sequentially by a control-volume-based method. The non-linear governing equations are discretized implicitly by a second-order upwind scheme and linearized to produce a system of equations for the dependent variables in every computational cell. The resulting linear system with a sparse coefficient matrix is then solved to yield an updated flow-field solution. The appropriate under-relaxation factors are imposed to avoid instability in the solution.

III. RESULTS AND DISCUSSION

The swirling motion of the fluid results in the pressure gradient being created in the radial direction, thus affecting the boundary layer development. The increased rate of heat transfer in such flows is a consequence of the reduced boundary layer thickness and increased resultant velocity. The radial distributions of the local axial velocity obtained in the experiment are shown in Fig. 3 under four different inlet velocities. In this figure, besides the swirling flow is shown, the radial distributions of local axial velocity of plug flow are also shown. It was found that the local axial velocity near the tube wall of swirl flow is more than that of the plug flow. It means the SERT can reduce the thickness of boundary layer. As it is shown in Fig 4, the local axial velocity near the tube wall at 10D is more than that at 60D. It means the swirl flow is decaying gradually along the tube.

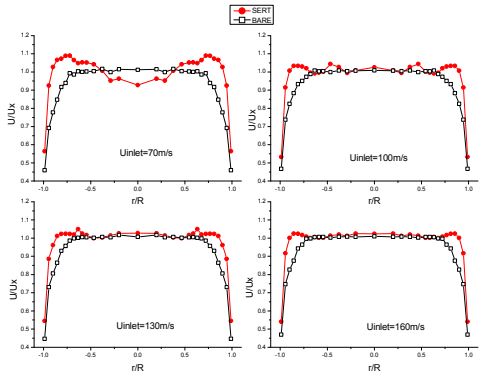

Figure 3. Comparison of the radial distributions of local axial velocity between SERT and bare tube.

From the Fig. 3 and Fig. 4, we can draw a conclusion that the SERT has significant impact on the flow in the tube. In other words, the SERT forced the plug flow to swirl flow in the tube.

CFD simulation can obtain detailed information on the velocity, pressure, and temperature in any point of the domain as shown in Fig 5 and Fig 6. By decomposing the calculated velocity into its components, it is clear the radial mixing effect that the SERT has on the flow. There is almost no tangential velocity in the tube before the SERT. The path lines that follow the direction of the flow can prove this point in Fig. 5, The flow is straight before the SERT, where in fact the tangential velocity is nearly 0. After the SERT, the velocity has a relevant tangential component, which enhances radial mixing in the tube. (Fig. 6)

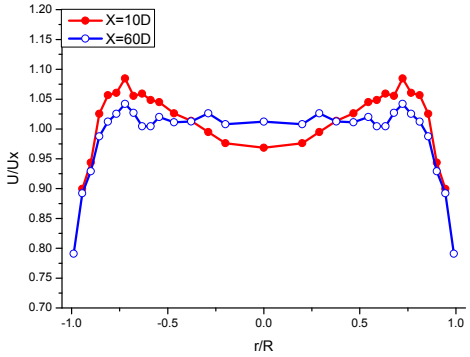

Figure 4. Comparison of the radial distributions of local axial velocity between at 10D and 60D

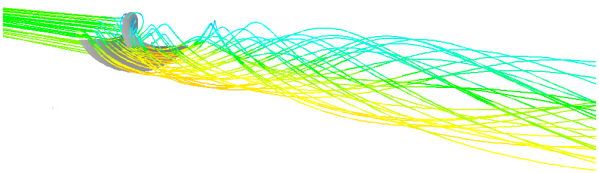

Figure 5. The path line in the SERT tube

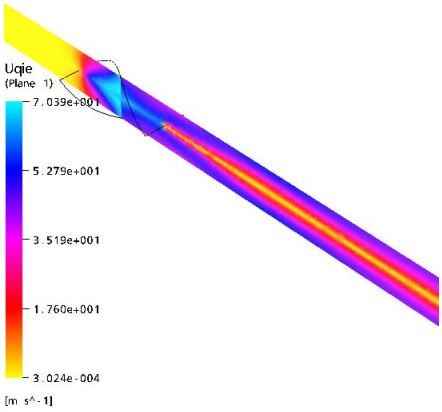

Figure 6. Tangential velocity in the SERT tube

The effect of the improved radial mixing is visible in the profile of temperature across the tube section. Figure 7 shows the radial profile of the flow temperature, T, over the cross sectional average, Tavg. For the SERT case, the profile is plotted at a distance of 3D downstream the SERT. It is clear that the temperature profile is much flatter for SERT case, resulting in a lower T next to the wall and a higher T towards the center of the tube.

The average tangential velocity profiles (Fig. 8) in SERT tube differs much from that in bare tube, but they are similar in the part far from the SERT section. The Nusselt number and heat transfer coefficient have the same trend as average tangential velocity (Fig. 9, Fig. 10). For the different inlet velocities, the high velocity has better performance in heat transfer process.

Just as mentioned above, the thermal cracking of hydrocarbons is always accompanied by coke formation, fouling the internal tube skin. This hampers the heat transfer towards the process fluid and reduces the diameter, increasing the pressure drop over the tube.

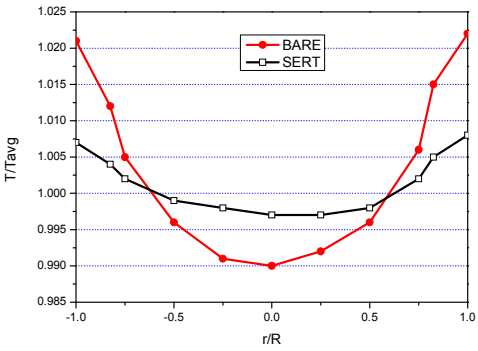

Figure 7. Comparison of fluid temperature between SERT and bare tube.

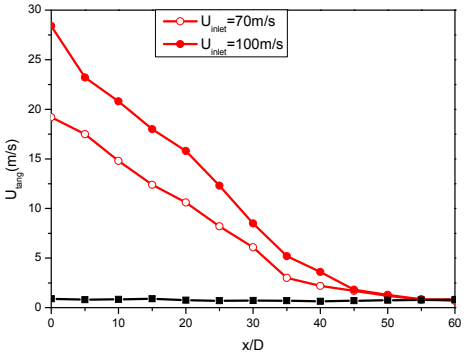

Figure 8. Comparison of tangential velocity in the SERT tube between two different inlet velocity.

It is well known that TMT is a function of the inside heat transfer coefficient and the thickness of coke layer. Based on above discussion, the SERT can increase the tangential velocity and inside heat transfer coefficient, and reduce the thickness of boundary layer and then alleviate the coke formation. Therefore, the TMT profile reflects the effect of the SERT on the furnace operation. Just as Fig. 11 shows, in the industrial furnace the TMT on the SERT tube increases slowly in the production cycle, on the contrary, the TMT on the bare tube increase sharply and the decoking of the furnace is carried out at the 55th day.

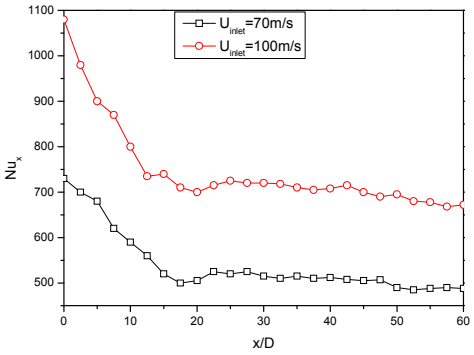

Figure 9. Comparison of Nu in the SERT tube between two different inlet velocities.

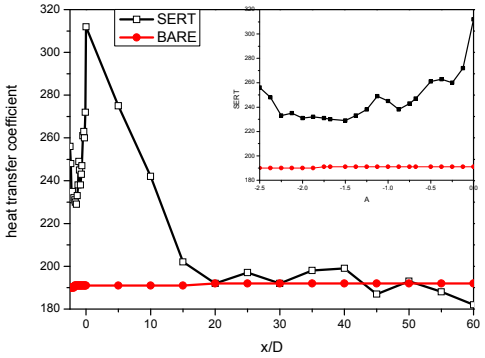

Figure 10. Comparison of heat transfer coefficient between SERT and bare tube.

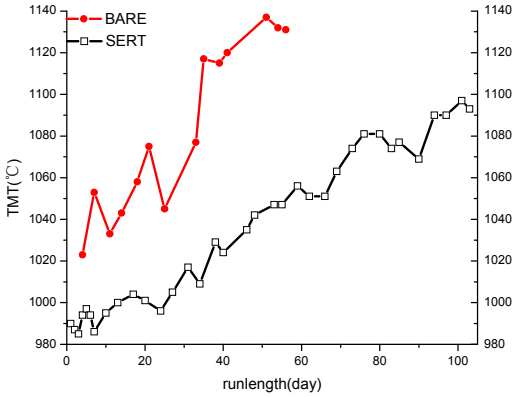

Figure 11. Comparison of TMT between SERT and bare tube.

IV. CONCLUSION

The SERT can be used to augment heat transfer rates, because the swirl flow augments the heat transfer and reduces the thickness of coke mainly due to the reduced the thickness of boundary layer and increased tangential velocity.

In the experiments, the result shows the plug flow is switched to swirl flow by SERT but the swirl flow is decaying along the tube far from the SERT. CFD is used to simulate the process of the flow and the heat transfer. The result shows the heat transfer is more efficient for SERT tube due to the more intensive mixing of the process fluid. Industrial experiments shows for the SERT tube, more even temperature profile and low thickness of coke layer are obtained, and this leads to longer product cycle of cracking furnace.

REFERENCES

[1] Lyle F. Albright, Billy L. Crynes, William H.Corcoran, pyrolysis: theory and industrial practice, Academic press, 1983.

[2] Hiroo Tominaga, Masakazu Tamaki, Chemical reaction and reactor design, John Willy&sons press, 1997.

[3] Geraldine J. Heynderickx and Gilbert F. Froment, A Pyrolysis Furnace with Reactor Tubes of Elliptical Cross Section, Ind.Eng.Chem.Res. 1996, 35, pp.2183-2189.

[4] Haiyong Cai, Andrzej Krzywicki, Michael C Oballa, coke formation in steam crackers for ethylene production, chemical engineering and processing, 2002, 41, pp.199-214.

[5] F.D.Kopinke, G.Zimmermann, G.C.Reyniers, G. F.Froment, Relative Rates of Coke Formation from Hydrocarbons in Steam Cracking of Naphtha. 3. Aromatic Hydrocarbons, Ind.Eng.Chem.Res. 1993, 32, pp.2620-2625.

[6] Geert C. Reynierst , Gilbert F. Froment, Frank-Dieter Kopinke , Gerhard Zimmermann, Coke Formation in the Thermal Cracking of Hydrocarbons. 4.Modeling of Coke Formation in Naphtha Cracking, Ind. Eng. Chem. Res. 1994, 33, pp.2584-2590.

[7] M. Yilmaz, O.Comakli, S. Yapici, enhancement of heat transfer by turbulent decaying swirl flow, energy conversion & management, 1999, 40, pp.1365-1376.

[8] Jeol magnan, Kaoru Hamada, kenji Otsubo, Elizabeth sohn, improved steam cracker furnace efficiency, petrochemical and gas processing, 2002, pp.125-129.